Atomistic resolution structure and dynamics of lipid bilayers in simulations and experiments

O. H. Samuli Ollila[1, *]

[1]*Aalto University*
(Dated: November 3, 2015)

Recent progress in the analysis of lipid bilayer atomistic resolution structure and dynamics using combination of robust experimental data and molecular dynamics simulations is reviewed. The focus is on order parameters and spin relaxation times measured with NMR and on form factors measured with SAXS and SANS for phosphatidylcholine lipid bilayers. The experimental observables are chosen since these experiments are robust, well understood, highly reproducible and the connection between raw data and simulations is straightforward. Also the comparison between simulations and these observables is bidirectionally useful; it will quantitatively measure the quality of the simulation model respect to the reality, and if the quality is sufficient, the simulations give structural interpretation for the experimental data. Significant advance of molecular dynamics simulation models is that the same simulation model can be simultaneously compared to all of this parameters. If satisfactory agreement is found, it is highly likely that the model represents the reality due to the large amount of reproduced independent experimental parameters. In this case all the mentioned experiments would be simultaneously interpreted with the same model. Phosphatidylcholine lipids are chosen since large portion of model membrane studies have been focused on this lipid, producing enough experimental and simulation data to draw comprehensive picture on the level of understanding atomistic resolution structure and dynamics. We conclude that the acyl chain region structure and its changes are generally well described in simulations, in contrast to the glycerol backbone and choline. Also cation binding is significantly overestimated by several models.

INTRODUCTION

1.Samuli: Add citations to the introduction. Rewriting is also needed Atomistic resolution molecular dynamics simulations of lipid bilayers are nowdays widely used technique to seek answer to various research questions. Typically interactions between other biological molecules (e.g. proteins, drugs, ions etc.) and lipids are studied but sometimes also lipid properties are directly under interest. The questions are often biologically motivated and the atomistic resolutions simulations gives very detailed information which is experimentally unattainable.

When simulations are used in this kind of studies, it is necessary to understand the limitations of the method and also the accuracy of the used model. In the pioneering atomistic resolution lipid bilayer simulations the quality of the simulation respect to reality was measured mainly by comparing the acyl chain order parameters and area per molecule between experiments and simulations. Especially some simulation models repruced these amazingly well which led to the wide usage of these models.

Despite of the success of the models to reproduce the acyl chain properties and molecular density more or less correctly, already early days it was pointed out by comparing simulations to various experiments that the glycerol backbone and choline headgroup order structure may not have been correctly described. However, at the time simulations were very short compared to currently accessible timescles and it was not clear if the molecules had time to sample all the states the model would predict. Also the method to quantitatively measure atomistic resolution molecular dynamics and compare to simulations was not available, thus the real sampling timescales were not known. For these reasons the estimates of the quality of headgroup were inconclusive on the early days of molecular dynamics simulations of lipid bilayers and the issue has gained more attention only very recently.

While the C-H bond order parameters for all hydrocarbon segments are yet the core parameter to quantify the lipid model quality, the area per molecule is quite generally replaced with form factor. The main reason is that the area per molecule is calculated from the scattering data using a model (set of assumptions). Thus, when this value is compared to the value from simulations, the simulations are not compared directly to experiments but to a value which comes from another model (set of assumptions to calculate the area per molecule). For this reason the area per molecule is nowdays replaced by comparison between form factor from simulations and x-ray or neutron scattering.

In this review we discuss the current state of the art methods to compare the atomistic resolution lipid structure and dynamics in simulations to the experiments. The C-H bond order parameters measured with NMR and form factors measured with x-ray or neutron scattering are discussed for structural comparison, and spin lattice relaxation rates for the comparison of dynamics. The main advantages of these parameters are that the experimental techiques are non-invansive, they are measured from multilamellar phase which is practically always present in simulations as well due to periodic boundary conditions and that the compared quantity (order parameter, spin lattice relaxation and form factor) is achieved from the actual experimental data in a robust way. The experimental results from these experimental techniques are also highly reproducible and the measured timescales are appropriate for the comparison to simulations. Also several other experimental parameters and techniques are used to quantify the simulation quality, however, none of these is as robust as order parameters, spin relaxation rates or form factor. The most commonly used other techniques are shortly discussed in the end of the review.

In this review we focus on phosphatidylcholine (PC) lipids

which has been in the focus of fundamental structural lipid studies for several decades now. However, there is a lot data available and the basis of our approach applies to other lipid types as well [?].

C-H BOND ORDER PARAMETERS AS ATOMISTIC RESOLUTION STRUCTURAL MEASURE

2.References should be added, the text should polished, things should be added and checked and figures should be improved. However, the main strucutre and idea of the section should be visible.

Definition and properties of C-H bond order parameter

In lipid bilayer systems the order parameter of a hydrocarbon C–H vector is typically defined as

$$S_{\mathrm{CH}} = \frac{1}{2}\langle 3\cos^2\theta - 1\rangle, \qquad (1)$$

where the angle brackets denote an ensemble average over the sampled conformations, and θ is the angle between the C–H bond and the membrane normal. The numerical values of order parameters vary between $-\frac{1}{2} < S_{\mathrm{CH}} < +1$ depending on the sampled θ distribution. The definition is motivated by its connection to the dipolar and quadrupolar splitting measured with ^{1}H-^{13}C and ^{2}H NMR techniques, respectively. The functional form comes from the fundamental theory of interactions between spin systems which gives a connection between average molecules orientations and NMR measurables [1].

If the sampled distribution of θ for a C–H bond are known, the order parameter can be straighfowardly calculated from Eq. 1. However, the sampled θ distribtions cannot be uniquely determined from the known order parameter. Thus the experimental order parameter values gives a set of conditions which structural molecular model (more specifically the C–H bond vectors of the model) has to fulfill but the experimental order parameters alone cannot be used to uniquely resolve the structure. The same applies practically to all experimental parameters used in biomolecular structure determination.

Atomistic resolution molecular dynamic simulations naturally produces the sampled structures from which the θ distributions can be calculated and used in Eq. 1 to calculate the order parameters. The sampled structures in the simulation can considered to be realistic only if the experimental order parameters are reproduced. If this is the case, the simulation can be then considered as an atomistic resolution interpretation of experimental order parameters. Before MD simulations were feasible for such usage, other models have been used for this interpretation [2? ? –7]. It is important to note, however, that the sampled structures which reproduce the order parameters are not necessarily the correct ones since, in principle, several structural models can produce the same order parameters. Significant advance of the MD models compared to the traditional models is that the same MD structures

can be straightforwardly compared to other experimental observables in addition to order parameters, like ^{31}P chemical shift anisotropy [8], ^{31}P-^{13}C dipolar couplings [9] and scattering data [?]. This will significantly reduce the possibility of getting unrealistic structures reproducing correct order parameters.

The probability for unrealistic structures with correct order order parameters is further reduced by the detailed and accurate experimental data available for order parameters. Order parameters are known with high quantitative accuracy for each C-H bond present in the lipid molecule for several lipid types [10? –15]. The absolute values of order parameters can be measured two independent techniques by using either ^{2}H NMR [16] or ^{1}H-^{13}C NMR [12, 17–19] and the sign can be measured with two different ^{1}H-^{13}C NMR techniques [7, 17, 18]. It is also possible that two hydrogen bonds in the same carbon has different order parameters (*forking*) which can be detected with both ^{2}H NMR [20? , 21] and ^{1}H-^{13}C NMR [?] techniques. As a result, for example for POPC lipid molecule in lipid bilayer there is ? order parameter numbers known experimentally and a structural model for this lipid should reproduce all of these. If some the order parameters are not reproduced, it is easy to detect the weak parts of the model since a single order parameter is very local quantity depending only on the position of two atoms (C-H pair). This is an advance over several other accurately measured NMR quantities, like ^{31}P chemical shift anisotropy [8] and ^{31}P-^{13}C dipolar couplings [9] which depend on the position of several atoms, thus in the case of disagreement, it is more difficult to pinpoint the problems in the model.

Order parameters from ^{2}H NMR experiments

The absolute values of order parameters are connected to the quadrupolar splitting $\Delta\nu_Q$ (^{2}H NMR) measured in ^{2}H NMR experiments through the equation

$$|S_{\mathrm{CD}}| = \frac{4}{3}\frac{h}{e^2 qQ}\Delta\nu_{\mathrm{Q}}, \qquad (2)$$

where e is the elementary charge, Q is the deuteron quadrupole moment and h is the Planck's constant. The parameter q is related to the largest electric field gradient and in practise its value is not known; therefore the static quadrupolar coupling constant $\frac{e^2 qQ}{h}$ is defined, and its value measured for different compounds in their solid state ($\Delta\nu_Q$ measurement from the system where order parameter is known to be 1). In C-D order parameter measurements for lipids, it is typical to use the value measured for different alkenes, $\frac{e^2 qQ}{h}$=170 kHz. The relation between order parameters and quadrupolar splittings then becomes $S_{\mathrm{CD}} = 0.00784 \times \Delta\nu_{\mathrm{Q}}$. This relation is useful as many publications report only the quadrupolar splittings. For a review and more accurate description see the work of Seelig [16].

Order parameters from ^{13}C NMR experiments

To determine order parameter with ^{1}H-^{13}C NMR experiments, the dipolar splitting $\Delta\nu_{\mathrm{CH}}$ is measured. This is then related to the effective dipolar coupling d_{CH} through a scaling factor depending on the pulse sequence used in the experiment [12, 17–19]. The effective dipolar coupling d_{CH} is connected to the absolute value of order parameter through equation

$$|S_{\mathrm{CH}}| = (\frac{D_{\max}}{2\pi})^{-1} d_{\mathrm{CH}}, \qquad (3)$$

where $D_{\max} = \frac{\hbar\mu_0\gamma_h\gamma_c}{4\pi\langle r_{\mathrm{CH}}^3\rangle}$. r_{CH} is the C-H distance, μ_0 is the vacuum permittivity, and γ_h and γ_c are the gyromagnetic constants for ^{1}H and ^{13}C nuclei. In contrast to Eq. 2, all the parameters in Eq. 3 are in principle known. However, for the internuclear distance only the average r_{CH} is known, not the third moment r_{CH}^3. For this reason values between 20.2-22.7 kHz are used for $\frac{D_{\max}}{2\pi}$ depending on the original authors [12, 17–19, 22, 23].

Quantitative accuracy of experimental order parameter values

It must be stressed that ^{2}H NMR and ^{13}C NMR are fully independent experiments since the deuterium quadrupolar splitting $\Delta\nu_Q$ and the dipolar splitting d_{CH} are different physical observables. In addition, the prefactors connecting the observables to the order parameter (Eqs. 2 and 3) are independently measured. Further independent experiments are performed With ^{13}C NMR by measuring the ^{1}H-^{13}C dipolar couplings using different pulse sequences [12, 17–19] when the connection between dipolar splitting d_{CH} and effective dipolar coupling d_{CH} is different.

The measurements of quadrupole $\Delta\nu_Q$ and dipolar d_{CH} splittings are relatively accurate, especially for quadrupolar splitting. **3.How accurate exactly?** Thus the quantitative accuracy of measured order parameters is mainly determined by the prefactors connecting the measured splittings to the order parameters (Eqs. 2 and 3). Since the prefactors are independently determined for the ^{2}H and ^{13}C NMR measurements, the quantitative accuracy is best estimated by comparing the independtly measured order parameter values.

The comparisons between order parameters measured with ^{2}H NMR and ^{13}C NMR by several authors shows very good agreement [12, 15, 18, 19]. Botan et al. collected literature values for PC lipid choline headgroup and glycerol backbone order parameters and concluded that order parameters would be known with the accuracy of ±0.02 for these segments in purified PC lipid bilayer samples [15] which agrees with the estimate of Gross et al [18]. The lower order parameter reported in some studies [7, 17, 24] were suggested to arise from lower experimental accuracy. The values collected by Botan et al. and the suggested sweet spots where choline and glycerol backbone order parameters should fall in the simulation models are shown in Fig. 1 A).

Acyl chain order parameters from different techniques are compared in Table 1 by Gross et al. [18], Dvinskikh et al. [12] and Ferreira et al. [19]. The comparison by Ferreira et al. [19] is also shown in Fig. 1 C). Generally good agreement between different methods is seen also for acyl chain order parameters, however, for some segments the 0.02 accuracy might not be achieved. **4.Maybe specify to which ones?**

Qualitative accuracy of experimental order parameter values

When order parameters are measured as function of changing condition (e.g. temperature, hydration level, ion concentration, etc.), the prefactors connecting the order parameter and the experimentally measured couplings can be considered to be unchanged. Therefore, accuracy of the measured change is determined by the accuracy of the splitting measurement in contrast to the previous section. Here we refer to this as a qualitative accuracy. Due to the high resolution of splitting measurements, especially in 2H NMR, the qualitative accuracy is much higher than the quantitative accuracy discussed in previous section.

The high qualitative accuracy of ^{2}H NMR experiments is exemplified in Fig. 2 by using the the classical experiment by Akutsu and Seelig [25], where the effect of different ions on the quadrupolar splittings of choline headgroup α and β segments was measured, [118] see Fig. **??**. The effects of different ions on the quadrupole splittings are clearly differentiable with the experimental accuracy in Fig. **??** A). However, when transformed to the order parameter units, these changes correspond only changes below 0.03 units for β and 0.05 for α as shown in Fig. **??** B).

As another example of the high qualitative accuracy of order parameter experiments, the measured order parameters for β and α carbons as a function of hydration level for different PC lipids are shown in Fig. 3. Quantitative numbers from different experiments show slight variation between different temperatures and lipid compositions. However, in all experiments the order parameters increase with decreasing hydration. [119] The smallest order parameter change is only slightly above 0.01 units, measured by Dvinskikh et al. with 13C NMR [41], demonstrating that high qualitative accuracy can be also achieved with 13C NMR.

In conclusion, the experimental qualitative accuracy order parameter measurements is very high. It is much higher than the accuracy achieved with state of the art MD simulations. Thus, the accuracy order parameter change comparison between simulations and experiments is limited by the simulation accuracy, not experimental.

On the other hand, it should be noted that since even very small splitting changes can be detected experimentally one should always connect these to the changes in real molecules to avoid overinterpretation. For example, it has been measured that cholesterol induces a measurable change (less than 2 kHz) in quadrupolar splitting [43]. This may tempt to con-
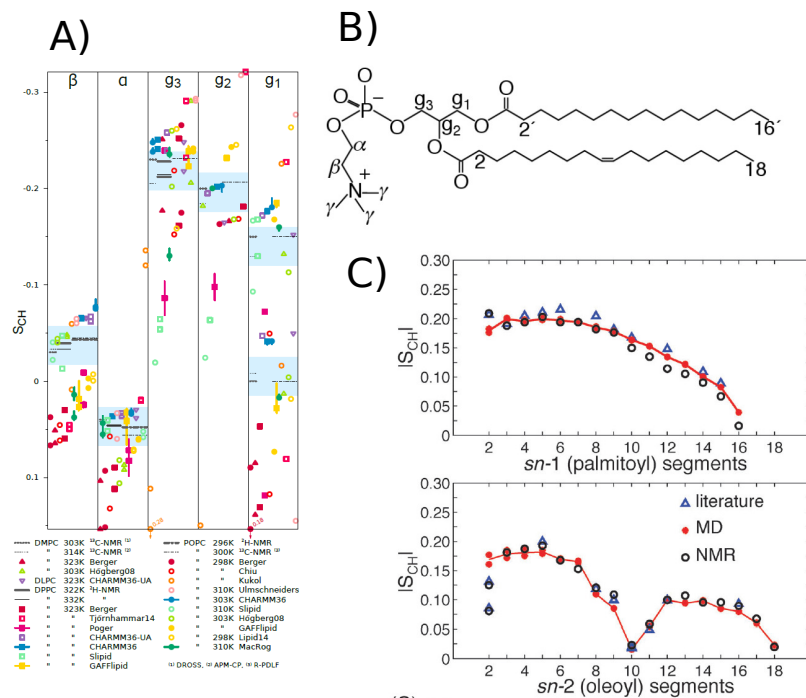
FIG. 1: A) Order parameteres from simulations and experimental values from literature for glycerol and choline groups collected by Botan et al. [15]. The experimental values were taken from the following publications: DMPC 303 K from [18], DMPC 314 K from [12], DPPC 322 K from [2], DPPC 323 K from [25], POPC 296 K from [26], and POPC 300 K from [19]. The original citations for the force fields used in the simulations are Berger [27], Hogberg08 [28], Poger [29], Ulmschneiders [30], Kukol [31], Chiu [32], CHARMM36 [33], GAFFlipid [34], Slipid [35], MacRog [36], Tjörnhammar14 [37], Lipid14 [38], CHARMM36-UA [39]. The vertical bars shown for some of the computational values are not error bars, but demonstrate that for these systems we had at least two data sets (see Table 1 in Botan et al. [15]); the ends of the bars mark the extreme values from the sets, and the dot marks their measurement-time-weighted average. The interactive version of this figure is available at https://plot.ly/~HubertSantuz/72/lipid-force-field-comparison/. B) Chemical structure of 1-palmitoyl-2-oleoylphosphatidylcholine (POPC). C) Picture adapted from [19]. Order parameter magnitude $|S_{CH}|$ vs. carbon segment number for the sn-1 and sn-2 acyl chains of POPC (A and B respectively). Data from fully hydrated POPC at 300 K obtained with ^{1}H^{13}C solid-state NMR (black dots) [19] and MD simulations (red dots) [19], as well as data from 2H NMR (blue triangles) (sn-1 [4] and sn-2 [4, 40] at 300 K).

clude that cholesterol affects to the choline structure, however, this quadrupolar splitting corresponds 0.016 unit change in the order parameter which indicates almost negligible conformational change [15].

Signs of order parameters

While only the absolute values of order parameters are accessible with ^{2}H NMR, two different ^{1}H-^{13}C NMR techniques allow also the measurement of the sign: first Hong et al. first measured order parameter signs for eggPC [17] and

DMPC [7]; then later Gross et al. used a different NMR technique to measure signs for DMPC [18]. All the experiments report negative order parameters for almost all the segments, only α and γ are positive.

Furthermore, the signs [7, 17, 18] and magnitudes [15, 19, 20] of choline headgroup and glycerol backbone order parameters are practically unaffected by the acyl tail contents of the bilayers. Thus, it can be fairly assumed that the order parameter signs for these segments are the same in all PC lipids in bilayer. On the other hand, the positive signs for g_1, g_3 and C_2 has been reported by Aussenac et al. [44] which has led to some confusion in comparison between simulations and
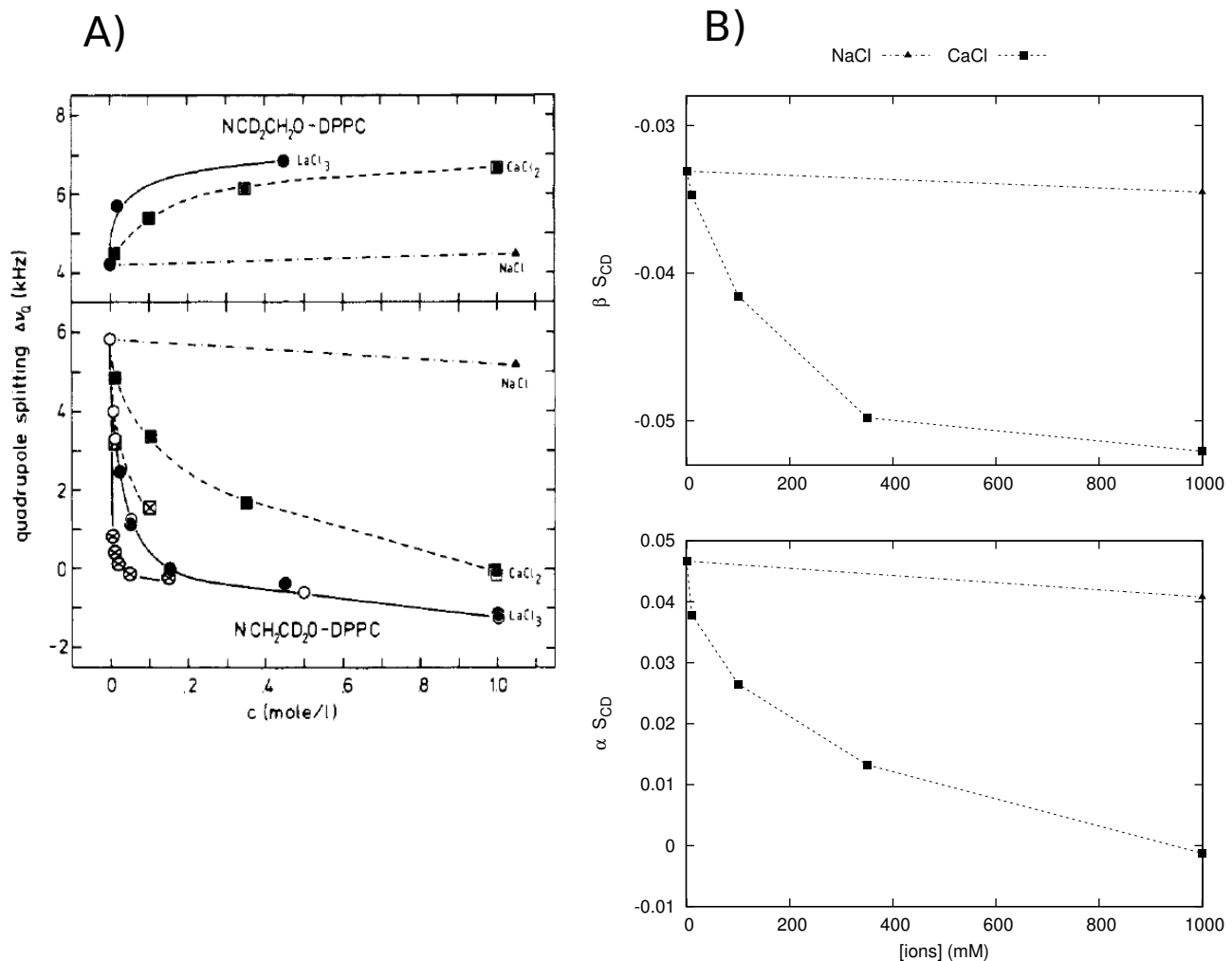
FIG. 2: A) Quadrupolar splittings as function of different ion concetrations measured by Akutsu and Seelig with ^{2}H NMR [25]. B) The data from A) translated to order parameters ($S_{CD} = 0.00784 \times \Delta\nu_Q$). Also the sign of β order parameter is put negative according to more recent experiments [7, 17, 18] (see also Ref. [15] and Section 4).

experiments [28]. However, these signs are not directly measured but extracted from the model used to interpret ^{2}H NMR order parameters from DMPC bicelles. Thus, it is reasonable conclude that order parameters are negative for all segments except for α and γ, as directly measured with ^{1}H-^{13}C NMR [7, 17, 18].

Even though the sign was not measurable with ^{2}H NMR, the sign was believed to be negative for acyl chains because θ was expected to fluctuate around 90° leading to negative order parameters [16]. This was later confirmed by using ^{13}C NMR measurements [17]. Also MD simulations always produce negative order parameters for acyl chains.

Typically when the response of order parameters to varying conditions (ions, dehydration and cholesterol) is measured, only the absolute values are reported [19, 25, 26, 41, 42, 45]. Where clear responses are observed, like with multivalent ions [25, 45] and dehydration [26, 41, 42], the experiments are done by gradually changing the conditions and the order parameter response is systematic, see Figs. 2 and 3. Thus, it

is reasonable to assume that also the signs are not suddenly changing. However, it seems that the sign of the α carbon order parameter does change in response to a large amount of bound charge, such as multivalent ions. In this case, the absolute value of the order parameter first decreases to zero and then starts to increase again [45, 46], as seen from the nicely illustrated spectra shown Fig. 4 by Altenbach et al. [45].

Forking of order parameters

It is possible that the CH$_2$ segment is sampling such orientations that the order parameters for different hydrogens in the same carbon have different values. We call this phenomena as *forking*, as done also previously to avoid confusion with splittings measured with NMR. The forking is detected with both ^{2}H NMR [4, 20?, 21] and ^{1}H-^{13}C NMR techniques [?] as two different quadrupolar or dipolar splitting values, respectively, related to the same CH$_2$ segment.

Exp. (DMPC ^{13}C T=314 K)[1] ---○---
Exp. (DOPC ^{2}H T=303 K)[2] ---□---
Exp. (POPC ^{2}H T=296 K)[3] ---△---

[1] Dvinskikh et al. PCCP 7, 3255 (2005)
[2] Ulrich et al. Biophys. J. 66, 1441 (1994)
[3] Bechinger et al. Chem. Phys. Lipids 58 1 (1991)

FIGURE 1: ^{2}H NMR spectra of coarse dispersions of POPC bilayers at various CaCl$_2$ concentrations (no NaCl). The lipid was deuterated at the α-segment ($-$NCH$_2$CD$_2$OP$-$). Measuring temperature, 40 °C.

FIG. 4: Quadrupolar splitting $\Delta\nu_Q$ of α of POPC as a function of CaCl$_2$ concentration, related to the order parameter as $S_{CD} = 0.00784 \times \Delta\nu_Q$. We know nowadays that the order parameter of α in the absense of CaCl$_2$ is positive [7, 17, 18]. Thus, the most obvious interpertation for the result is that the α order parameter decreases to zero when CaCl$_2$ concentration reaches 2.0M, and above these concentrations becomes increasingly negative with further addition of CaCl$_2$. Reprinted with permission from Altenbach and Seelig, Biochemistry, 23, 3913 (1984). Copyright 1984 American Chemical Society.
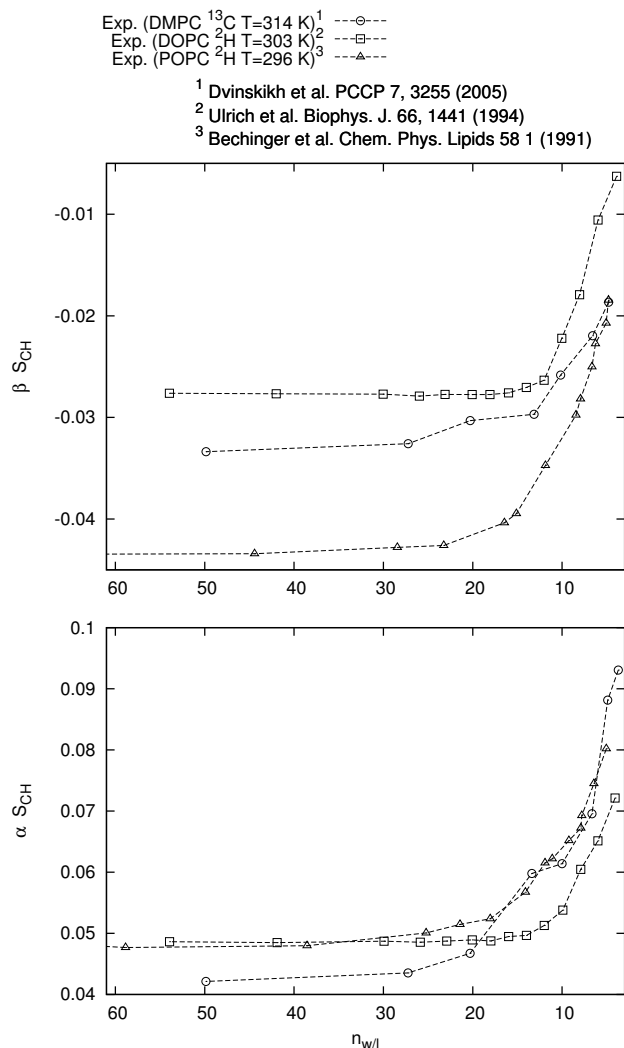
FIG. 3: Dehydration changes on α and β order parameters measured with different methods. The data taken from Dvinskikh et al. [41], Ulrich et al. [42] and Bechinger et al. [26] Also the sign of β order parameter is put negative according to more recent experiments [7, 17, 18] (see also Ref. [15] and Section 4).

The forking is observed for g_1, g_3, and C$_2$ carbon in the *sn*-2 chain segments in a fluid PC lipid bilayer, for other CH$_2$ segments the equal order parameters are observed for both hydrogens are equal [3, 4, 19?, ?, 20]. The forking has been studied in detail with ^{2}H NMR techniques by separately deuterating the R or S position in CH$_2$ segment to assign order parameters to correct hydrogens [20]. **5. Has this been done for the C$_2$ carbon in the *sn*-2 chain?**

^{2}H NMR studies also show that the forking really arises from differently sampled orientations of the two C–H bonds, not from two separate populations of lipid conformations [20, 21]. This means that realistic atomistic resolution molecular models has to reproduce the forking correctly. Thus, the simu-
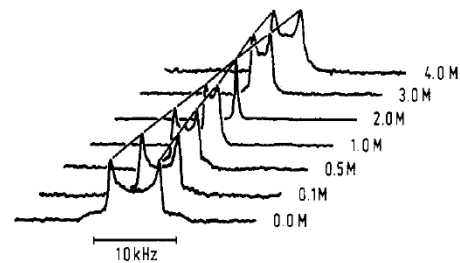
lated order parameters has to be calculated separately for each hydrogen by taking into account the isomeric position for the structural comparison to the experimentals. Recent work by Botan et al. shows that several simulation models has problems in this respect [15] (see also Fig. 1).

Order parameter values in the literature

For ^{2}H NMR measurements the CH$_2$ segments has to be labeled with deuterium. This can be done specifically for a certain segment or for the several segments simultaneously [?]. In the first case, it is known that the measured order parameter (quadrupolar splitting) is related to the labeled segment. In the latter case several order parameters (quadrupolar splittings) are measured which arise from all the labeled segments, however, it is not known which order parameter belongs to which segment. Majority of the ^{2}H NMR data in the literature is measured from samples with perdeuterated acyl chain [10] since the synthesis of specifically deuterated lipids is complicated [?] and they are expensive. From this kind of data alone one cannot know which order parameter is assigned to which CH$_2$ segment. On the other hand, also order parameter data from specifically deuterated lipids are available from several lipid types in various conditions [3, 4, 20?].

Specific labeling is not needed for order parameter measurement with ^{13}C NMR due the natural abundance of 13C, however it could be used to enhance the signal for specific segment under interest [?]. Order parameter measurements with ^{13}C NMR are 2D experiments, the chemical shift being in the first dimension and dipolar coupling in the second [?]. The chemical shift depends on the local chemical environ-

ment and is different for each carbon segment. In the second dimension the dipolar coupling (order parameter) corresponding each chemical shift value is measured, and its value can be connected, in principle, to each carbon segment by using the chemical shift value. In practise, challenges occur in the acyl chain region where chemical shift values of different segments are very close to each others [12, 14, 17–19]. This issue has been addressed by filtering the spectra by using partially deuterated lipids [19] and using data from simulations and specifically deuterated experiments to help in the assigment [14, 19]. It should be noted that the overlapping spectra is a challenge only for acyl chain regions with several similar segments. On the other hand, the order parameters for hydrocarbon segments in choline, glycerol backbone, close to the double bonds, and in the beginning and the end of acyl chains can be straighfordly measured from the natural abundance lipid samples.

The order parameters are typically measured from multilamellar samples which are good for comparison to MD simulations since it a nearest experimental correspondence for a simulation box with periodic boundary conditions. In this work we do not discuss order parameters can be measured also from other type of samples, e.g. bicelles [44, 47, 48], or indirect measurements by using, e.g. relaxation data [49] since their comparison to simulations is less straightforward.

The available experimental data for order parameters is reviewed quite recently [10, 11]. These reviews are comprehensive especially for acyl chains in pure lipid bilayer samples. In addition to this, there is significant amount of order parameter data for glycerol backbone and headgroup segments [15], and also data as a function of changing conditions for all lipid segments [12, 19, 25, 50**?**]. The amount of data, especially from ^{13}C NMR, has been also increasing lately [13, 14, 19]. Especially the order parameter data of headgroup responses to varying conditions has a lot of unused pontential since it can used to measure, e.g. ion partitioning to lipid bilayer [25, 51**?**] and lipid protein interactions [13, 52, 53]. Simultaneously, it gives accurate experimental parameters which can be directly compared to MD simulations [15, 51].

Order parameters from simulations

In atomistic resolution molecular dynamics simulations molecules are sampling the defined ensemble according to the used simulation parameters and the coordinates of each atom as a function of time are saved to the trajectory files. The coordinates in the trajectory file can be straighfordly used to calculate order parameters directly from the definition in Eq. 1. The average is taken over the molecules and time.

For simulations with united atom models without explicit hydrogen atoms [15, 54, 55], the hydrogen positions can be generated post-simulatively from the positions of the heavy atoms and the known hydrocarbon geometries. This can be done explicitly by creating a trajectory with added hydrogens [15, 54], or by using equations which directly calculate order parameters from heavy atom positions [55, 56]. For C-H and C-H$_2$ segments without forking these two approaches gives essentially identical results when applied correctly. However, the latter is valid only for the cases with no forking, i.e. order parameters are equal for both hydrogens attached to the same carbon. Since this is not known *a priori* for the analyzed model, it is better to use the first approach with explicitly added hydrogens.

The difference in the forking analysis is most likely reason for different choline and glycerol backbone order parameters reported in the literature for the same model [15, 57]. Also different order parameters from the same model for C-H bonds has been reported in literature [54, 58] which most likely arises from incorrect implementation of widely used version of *g_order* program in the Gromacs package for this segment. Also, the *g_order* program prints -S$_{CH}$ which is most likely the reason to the reported positive order parameters for acyl chains in some studies [59]. When these issues are taken into account, the order parameters from the same models reported in the literature are generally in good agreement.

The statistical error estimates for order parameters in simulations are estimated by using the error of the mean calculated averaging over time blocks [54], over independent simulations [57] and over different lipids [15]. The maximum error bars given by all these approaches are $\sim \pm 0.01$.

It was recently pointed out that the sampling of individual dihedral angles might be very slow compared to the typical (100 ns) simulation timescales [60]. This result raises a question if typical simulation time scales are long enough to allow the molecules to sample the full phase phase. On the other, another recent study showed that the slowest rotational autocorrelation function observed (for g$_1$ segment) in the Berger model reached a plateau (S_{CH}^2) after $\sim$200 ns and its relaxation was significantly too slow compared to NMR relaxation experiments [23]. This indicates that if the typical simulation times are too short for the full sampling of the structures, then the dynamics is unrealistically slow in the simulation model.

Comparison between order parameters from simulations and experiments

Since the early days of lipid bilayer simulations the acyl chain order parameters are commonly calculated and compared to experiments when validating simulation studies [27, 56, 61–71]. Practically all the state of the art force field parametrization publications report these to be in good agreement with experiments [8, 27–39]. It is remarkable that the experimental order parameters for acyl chains in fully hydrated pure lipid bilayers can be reproduced within experimental error, see also Fig 1 C).

Exception is the C$_2$ segment in *sn-2* chain in all PC lipids which is known to have measurable forking and lower magnitudes compared to other order parameters in the beginning of the acyl chain [**?**]. This important structural fingerprint is related to the different conformations between carboxyl seg-

ments in the beginning of chains [**?**]. This feature is, however, not analyzed or not reproduced for several lipid models [8, 28, 30–32, 34–37] while some models report the lower magnitude but the forking is not reproduced correctly or analyzed [8, 33, 38]. The united atom CHARMM36 is really close the experimental results [39].

In addition to the quantitatively good agreement in pure bilayers, the changes in acyl chain order parameters as a function of changing conditions are generally reasonable. For example, experimentally observed increase of order parameters as a function of cholesterol concentration [19, 55, 72**?**, 73] and with dehydration [41, 50] are reproduced in simulations [19, 55, 74–79]. However, systematic and quantitative comparisons of these effects between experiments and simulations are rare [19, 79]. Comparison between widely used model (Berger lipids [27] and Höltje cholesterol model [80] [120]) for cholesterol containing lipid bilayer revealed that even though the acyl chain response is reasonable, the simulation model cannot be considered to agree with experiments with 34% and higher cholesterol concentrations. CHARMM36 model has been shown to slightly underestimate the cholesterol ordering effect in DMPC bilayer [77], while Slipids [78] and Lipid14 [79] models show satisfactory agreement. Lipid14 is also compared to the same extensive experimental data for POPC/cholesterol as Berge/Höltje model [19] and the agreement is significantly better [79], see Fig. 5. Also the orientation of cholesterol itself is reasonable in all models [19, 55, 77, 79], however, the cholesterol acyl chain has some issues in Höltje model [19] (too low order parameters) and in Lipid14 [79] (significant forking) while CHARMM36 reproduces experiments well [77].

The decrease of acyl chain order parameters due to the addition of double bonds is also generally reproduced by different simulation models [19, 33, 34, 38, 39, 54, 58, 78, 81–89]. Very good agreement for oleyl chain in POPC bilayer with one *cis* double bond is demonstrated in Fig. 1 taken from Ferreira et al. [19]. Also the effect of multiple double bonds (polyunsaturation) [54, 58, 81, 82, 84–86, 88, 89] (see Fig. 6) and difference between *cis* and *trans* double bonds can be reproduced in MD simulations [90].

In contrast to acyl chains, the order parameters for the glycerol backbone are not routinely reported in simulation literature and when reported, the agreement with experiments is concluded to be poor [15, 57, 75] or good [28, 75, 93] depending on the authors. The difference arises from different estimations for the accuracy of experimental and simulated order parameters, see also section 2. The NMRLipids collaboration recently carefully compared glycerol backbone and choline order parameters from 13 different models to the experiments and concluded that none of the available models reproduces these within experimental error, see Fig. **??**. Also responses of glycerol backbone and choline order parameters to dehydration, cholesterol concetration and charge penetration were studied by the NMRLipids collaboration [15, 51]. Despite of the incorrect structures in simulation models the experimentally measured choline order parameter increase due to dehy-

dration [15] and decrease due to penetrating ions [51] (see Fig. 7) were qualitatively reproduced. The comparison reveals, however, that the Na+ penetration is significantly overestimated by many models [51]. Also the effect of cholesterol on glycerol backbone and choline was overestimated by the Berger/Hltje model while CHARMM36 and MacRog performed better [15].

In conclusion, the experimental order parameters for acyl chains and their changes are resonably reproduced all state of the art lipid models (except for C_2 segment in *sn*-2). However, all models have difficulties with varying severity to reproduce the glycerol backbone and choline order parameters, and their changes.

Interplay between simulations and NMR order parameters: Validation and interpretation

As reviewed here, the order parameters can be measured with high accuracy for each hydrocarbon segment in lipid in bilayer and the values are available in the literature for wide range of different lipids in different conditions. Thus, the experimental order parameters give very detailed and local information about the orientations sampled by each C–H bonds in the lipid bilayer system. The order parameters can be also calculated from MD simulations with high accuracy and compared to the experiments. If the order parameters agree within experimental error, the simulated structures can considered as an structural intepretation for order parameter experiments. On the other hand, if the agreement is not good, the simulation is sampling incorrect structures.

As discussed in the previous section, the order parameters for acyl chain region from MD simulations generally agree well with experiments (except for the C_2 segment in the *sn*-2 chain). Thus, the acyl chain structure is most likely realistic in simulations and they can used for structural interpretation for this region. This is a significant advancement to the traditional structural models build based on the fittings to the order paramters [**?**]. The dynamical visualization of simulation trajectory immediately reveals very dynamical nature of acyl chains, rapidly sampling large amount of different conformations (for dynamics see the Section **??**). These videos published by several authors in supplementary information [**?**] gives significantly better intuitive understanding of dynamical nature of lipid bilayers compared to the static ones from traditional models. Since the lipid bilayers can be considered as a simplistic models for cell membranes and other biological lipid layers, this understanding has significant impact on biophysics and biochemistry.

Also the order parameter changes with changing conditions are qualitatively reproduced in the acyl chain region, however the systematic quantitative comparison of changes is rare [19, 54, 79]. The MD simulations have been especially useful to explain the origin of order parameter decrease due to *cis* double bonds in the acyl chain [54, 58, 85, 86, 94–96]. The order parameter decrease might arise from reduced order of
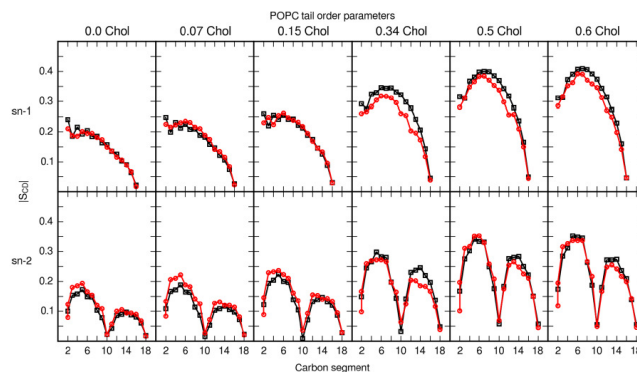
FIG. 5: Cholesterol effect on acyl chain order parameters compared between ? model [79] and experiments [19]. The agreement with experiments with this model is significanly better than Beger/Höltje based model compared by Ferreira et al. [19].

the chain or from the changed average θ angle in Eq. 1. From NMR experiments alone it was impossible to judge which is the correct explanation for the decreased order parameters due double bonds [85, 86, 94–96]. Several simulation studies by different authors using different models has showed that the decreased order parameter order parameter due to *cis* double bonds can be reproduced by introducing proper dihedral potentials next to double bonds, and due to the fexility of these dihedrals the polyunsaturated acyl chain becomes more flexible and the order is reduced [54, 58, 86, 94–96]. These studies concluded that order parameter decrease due to double bonds arises from genuine disorder of the chain, not from the changes in average angle [95, 96]. This is a prime example of the case where MD simulations have significant advance over more traditional modeling approaches [95].

The increase of acyl chain order parameters and related bilayer thickening due to addition of cholesterol is also qualitatively reproduced by simulations giving also intuitive visualizations for these effects [19, 79 **?**]. However, quantitative comparison reviewed in previous section revels that some models do not reproduce the acyl chain order parameters within experimental error in cholesterol mixtures [19, 77]. This indicates that these models are not yet accurate enough to give atomistic resolution interpretation to delicate lipid cholesterol interactions which are known to induce liquid-ordereded and liquid-disordered phase coexistence [97]. The recent Amber model [79] seems promising in this respect, see also Fig. 5. Careful quantitative comparison of dehydration induced ordering effect has not been made but it is mentioned to be weaker in simulations compared to experiments [75].

Simulation studies have also predicted changes in the acyl chain region which are yet to be experimentally confirmed, e.g. order parameter decrease due to lipid oxidation and changes in order parameter sign in oxidized acyl chain [59].

As discussed in the previous section, simulations models are not able to reproduce the glycerol backbone and choline headgroup order parameters within experimental error [15] in contrast to acyl chains. Thus, even the state of the art simulation models are not able to resolve the sampled atomistic

resolution structure of these segments which has been also tremendeous challenge to the more traditional models [**?**]. Consequently, the conclusions made from MD simulations which depend on atomistic resolution structure of energetics of these segments should be taken with extreme caution. On the other hand, the qualitative response of choline α and β order parameters to the dehydration and penetrating ions (increase and decrease, respectively) was correctly reproduced by several models, despite of the incorrect structure in fully hydrated lipid bilayer [15, 51]. These changes could be related with the changes of P–N vector angle respect to the membrane normal as suggested previously in [**?**]: the tilting of P–N vector more parallel to membrane plane with dehydration leads to the increase of choline order parameters [15] and *vice versa* with penetrating ions [51]. **6.The analysis with ions not actually done yet!** The widely used Berger/Hltje model significantly overestimates the structural effects due to cholesterol in the glycerol backbone and choline regions [15, 19] which seems to be the case also for Lipid14 [79].

The recent progress in the NMRlipids collaboration has shown that simulations confirm the electrometer concept suggested by Seelig et al. in a serie of classical publications [**?**]: the decrease of α and β order parameters is a measure of charge penetrated in PC lipid bilayer [51], see also Fig, 7. The concept gives a direct and quantitative route to compare charge binding into PC lipid bilayers between simulations and experiments through the choline order parameters [51]. While experimental results show only very weak or negligible Na^+ binding, some simulation models predict significantly stronger binding, see [51] and Fig. 7. This is a serious artefact since specific cation binding makes a lipid bilayer positively charged, which has a potential to lead incorrect conclusion when interactions with charged objects are studied. Thus the numerous conclusions from simulation studies with strongly binding Na^+ has to be taken with extreme caution. In contrast to monovalent ions the Ca^{2+} and other multivalent ions significantly partition to PC bilayers [**?**]. This is also seen in simulations, however, the structural effects are overestimated at least in the Berger model [51]. The CHARMM36 behaves
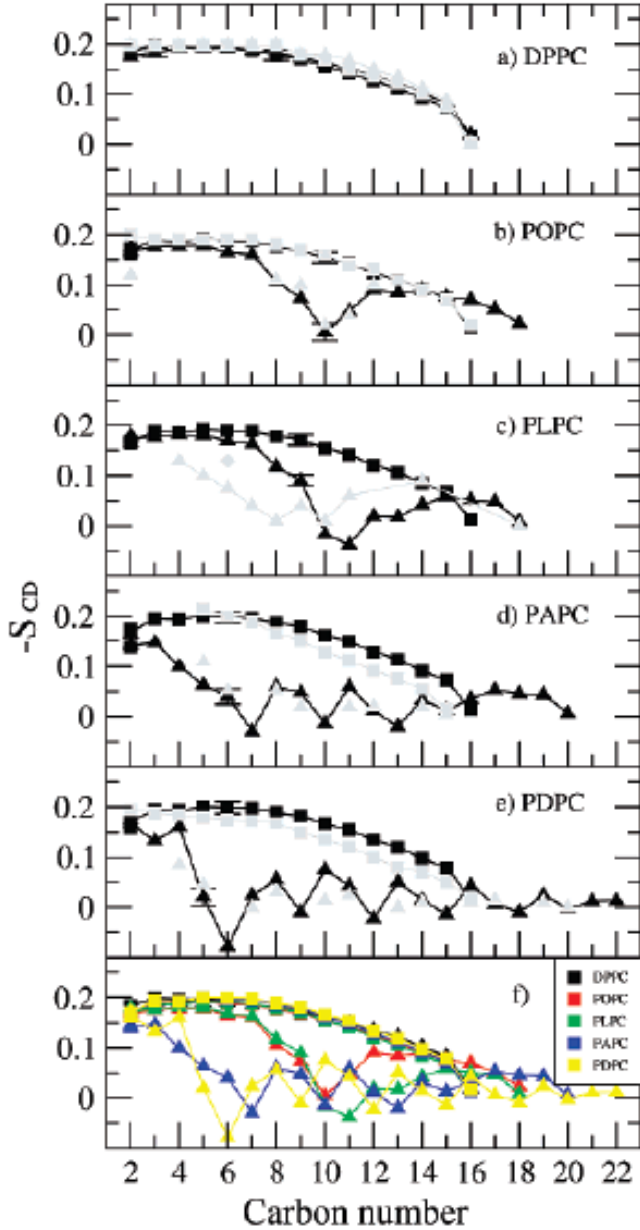
FIG. 6: Figure comparing order parameters in polyunsaturated acyl chains between simulations and experiments taken from [54]. Order parameters for the sn-1 (squares) and sn-2 (triangles) chains of (A) DPPC, (B) POPC, (C) PLPC, (D) PAPC, and (E) PDPC. Simulation results are shown in full black, and experimental results for comparison in gray. Additionally, part F summarizes the data for all bilayers from the simulations. Experimental order parameters were chosen for comparison as follows. The order parameters for DPPC (T=323K) are based on studies by Petrache et al. [91] whereas the experimental S_{CD} values for PDPC and for the sn-1 chain of POPC (T=310 K) are based on studies by Huber et al. [85] For the sn-1 chain of PDPC, the data set at 310 K is obtained by linearly interpolating between data at 303 and 323 K, whereas for the sn-2 chain the data at 303 K are presented [85]. Experimental values for the sn-2 chain of POPC are based on studies by Seelig et al. [4] A single experimental value is available also for the sn-2 chain of the PLPC bilayer at 313 K (diamond) [6] to compare with our simulated order parameters for PLPC. Together with PLPC, there are also experimental results for PiLPC (T=313K) [6]. Experimental order parameters for the sn-1 and sn-2 chains of PAPC (T=303 K) are based on quadrupole splittings measured by Rajamoorthi et al. [92]. For the sn-1 chain the monotonic decrease through the acyl chain is expected. For the sn-2 chain, values are fitted such that the agreement is as good as possible.
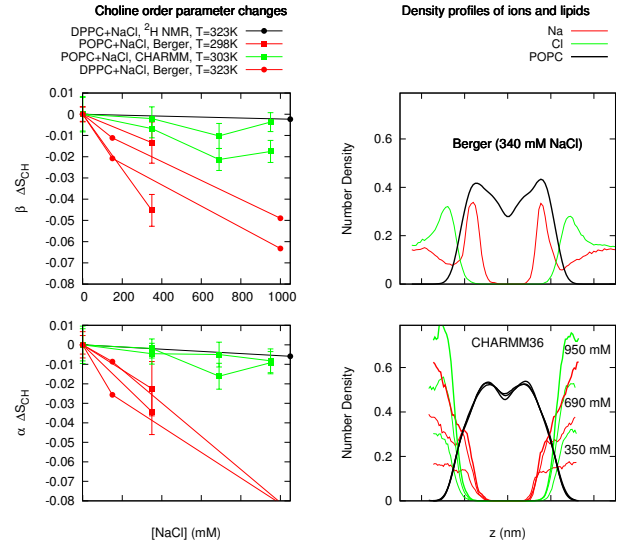

FIG. 7: Changes in order parameters as a function of Na+ concentration (left column) and ion density distributions (right column). With Berger model significant order parameter reduction and ion partition is observed while with CHARMM36 modest order parameter change and ion parition observed. The results confirm the concept by Seelig et al. which allows the ion partition to be measured by changes in α and β order parameters. The results clearly show that Berger model has too strong Na partition. For more discussion see [51].

more realistically, however, more careful simulation studies are needed to conclude if some of the existing models in capable to correctly reproduce PC ion interactions [51].

In conclusion, the atomistic resolution MD simulations are invaluable in understanding the structural details and their changes in acyl chain region, especially for double bonds. However, serious artefacts are possible, or even likely, in simulations studies where choline or glycerol backbone structure, or cation binding are important.

C-H BOND ROTATIONAL DYNAMICS FROM SPIN RELAXATION RATES AND SIMULATIONS

7.This is the first sketch of this section. A lot of references should be added, the text should be polished, things should be added and checked and figures should be improved. However, the main strucutre and idea of the section should be visible.

Definition and properties of rotational autcorrelation function

The second order auto-correlation function for the reorientation of the C–H chemical bond axis is defined as [98]

$$g(\tau) = \langle P_2[\vec{\mu}(t) \cdot \vec{\mu}(t + \tau)]\rangle, \qquad (4)$$

where P_2 denotes the second Legendre polynomial, $P_2(\xi) = 1/2(3\xi^2 - 1)$, $\vec{\mu}(t)$ is the unitary vector having the direction

of the C–H bond at time t, and the angular brackets denote a time-average. This autocorrelation is usually chosen to describe the C–H bond rotational dynamics since it is connected to the experimentally measurable spin relaxation rates through its Fourier transformation called spectral density

$$j(\omega) = 2 \int_0^\infty \cos(\omega\tau)g(\tau)d\tau. \tag{5}$$

In this review we focus only on experiments measured from multilamellar samples with randomly oriented sheets, thus only the second order auto-correlation function is needed [**?**].

In randomly oriented multilamellar samples the auto–correlation function of bond orientations always decays to zero with long enough time scales. However, the relaxation timescales can be divided to two distinct timescales. First the relaxation processes shorter than microsecond timescales occurs when lipid molecules are reorienting in the lipid bilyer but are not essentially moving between lipid bilayer regions with different orientations. Then with larger than microsecond timescales the movement between differently oriented bilayer regions decays the rotational correlation function to zero. In addition, MAS experiments the sample spinning causes lead orientaitional relaxation in kHz region. The full auto–correlation decaying to zero is illustrated in Fig. 8. Due to the timescale separation the correlation function can be written as [99]

$$g(\tau) = g_{\mathrm{f}}(\tau)g_{\mathrm{s}}(\tau); \tag{6}$$

$g_{\mathrm{f}}(\tau)$ describes the decay of $g(\tau)$ due to fast molecular motions and $g_{\mathrm{s}}(\tau)$ contains the contribution from slower motions

$$g_{\mathrm{s}}(\tau) = e^{-\frac{\tau}{\tau_{\mathrm{s}}}}\left[\frac{2}{3}\cos(\omega_R\tau) + \frac{1}{3}\cos(2\omega_R\tau)\right], \tag{7}$$

where τ_s is a correlation time due to slower isotropic molecular motions originating from the diffusion between bilayers with different orientations of their principal symmetry axis, and the cosine terms are the contribution from magic angle spinning of the sample, rotating at $\omega_{\mathrm{R}}/2\pi$ cycles per second [100], typically in the kHz frequency range.

The order parameter measurements with ^{2}H NMR and ^{13}C NMR measure the bond order after the relaxation of rotational motion inside the bilayer plane but before the relaxation between different bilayer orientations, as illustrated in Fig. 8. In typical molecular dynamics simulations with periodic boundary conditions the lipid molecules are restricted to single bilayer orientation and also the timescales are currently typically below microsecond. In these simulations the auto–correlation function in Eq. 4 decays to the square of order parameter in Eg. 1 in bilayers with planar symmetry, i.e. no microscopic phase separation of defects present. Also this is illustrated in Fig. 8.

The rotational correlation function describes how long does it take for a single molecule on average to sample the confor-
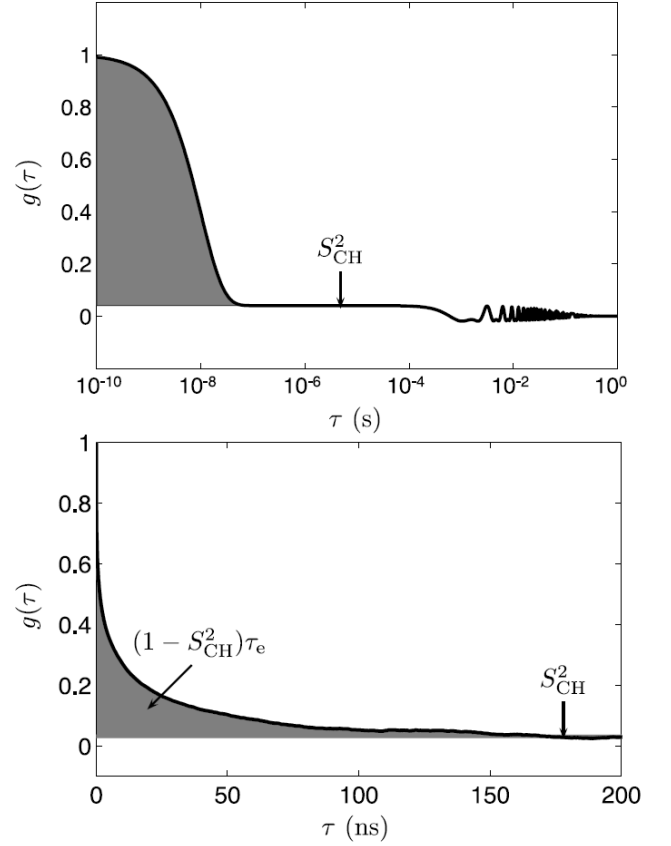

FIG. 8: (Top) Illustration of the auto-correlation function $g(\tau)$ and effective correlation time τ_e for a 13CH bond in a lipid bilayer in MAS experiment (x–axis with logarithmic scale). Plateau after short timescale relaxation processes $(g(\tau)_f)$ is shown between roughly 10^{-7}s and 10^{-4}s. After this timescale the slow relaxation processes $(g(\tau)_f)$ and oscillation due to MAS (Eq. 7) are shown. (Bottom) Example of $g(\tau)$ from a united-atom MD simulation of a POPC bilayer in excess water, illustrating the decay towards S_{CH}^2 (x–axis with linear scale). This represents the $g(\tau)_f$ in Eq. 6 and decrease to the plateau in the top figure. The effective correlation time τ_e is equal to the area in gray scaled by $(1S_{\mathrm{CH}}^2)^1$. Figure adapted from [23]

mations. The effective correlation time

$$\tau_e := \int_0^\infty \frac{g_{\mathrm{f}}(\tau) - S_{\mathrm{CH}}^2}{1 - S_{\mathrm{CH}}^2}\mathrm{d}\tau \tag{8}$$

can be used as an intuitively useful single parameter to describe this time. The larger this parameter is, the longer it takes in average to sample the conformations related to the bond. With this definition the area between the correlation function and its pleateau becomes $(1 - S_{\mathrm{CH}}^2)\tau_e$.

Detecting C–H bond dynamics experimentally

The most used parameter to detect the C–H bond dynamics experimentally in time scales comparable to simulations

are the spin-lattice relaxation rates R_1 from deuterium labels and ^{13}C. R_1^C measured from ^{13}C is connected to the spectral density (Eq. 5) through the equation

$$R_1^C = \frac{D_{\max}^2 N_H}{20} \left[j(\omega_H - \omega_C) + 3j(\omega_C) + 6j(\omega_C + \omega_H) \right], \quad (9)$$

where ω_C and ω_H are the Larmor angular frequencies of ^{13}C and ^{1}H respectively, N_H is the number of bound protons and $\frac{D_{\max}}{2\pi} \approx 22$ kHz as in section 2. R_1^D measured from ^{2}H is connected to the spectral density (Eq. 5) through the equation

$$R_1^D = \frac{12\pi^2}{40} \left(\frac{e^2 qQ}{h} \right)^2 \left[j(\omega_D) + 4j(2\omega_D) \right], \quad (10)$$

where $\frac{e^2 qQ}{h} = 170$kHz as in the case of order parameters in section 2.

Also the model free approach to measure the effective correlation time (Eq. 8) was recently introduced [23]. The method is based on the combination of experimental order parameter S_{CH}, spin-lattice relaxation rates R_1 and the transverse magnetization under a spin lock pulse $R_{1\rho}$ with measured appropriate nutation frequency through equation

$$\tau_e \approx \frac{5R_{1\rho}^{\text{plateau}} - 3.82 R_1^C}{D_{\max}^2 N_H (1 - S_{CH}^2)}. \quad (11)$$

Analyzing C–H bond dynamics from simulations

As in the case of order parameters, the auto–correlation function for each C–H bond can be calculated directly from simulations using the definition in Eq. 4 since the trajectories of each atom is known as a function of time. As in the case of order parameters the positions of hydrogens can be determined for united atom models based on heavy atom positions and assuming tetrahedral configurations [23, 101, 102]. Usually in the correlation function calculation all the available time intervals from the simulation data are used and the average over those and all molecules is taken. However, since the amount of data decreases when the the time interval approaches the total length of the simulation, usually the largest time interval used is the half of the total simulation length, for more details see [103].

To connect the auto–correlation functions from simulations to the experimentally measurable spin lattice relaxation times, the spectral density (Eq. 5) must be first calculated. In principle, this could be done using numerical fourier transformations techniques, however this often leads to unneccessarily large fluctuations. Instead, commonly used apporach is to fit analytical functional form to the calculated auto–correlation function and then use analytical Fourier transform of the fitted function [23, 101, 102, 104, 105]. Most commonly the sum of 4 or more exponentials is used as a fitting function [23, 54, 94, 104–106] but also streched exponential has been used [101, 102]. Numerically the functional form

of the fitting function should not matter as long as the fit is good, however, theoretically the correct correlation function form to describe the modes of physical motion can be debated [10, 102, 107–109]. It is clear from correlation functions from simulations that one exponential is not enought to produce a good fit while 4 gives a reasonable fit [94]. This is not surprising since more than one relaxation timescale is definitiely expected to be present in lipids in bilayer [10, 104–106].

After the fitting the analytical form of the spectral density predicted by simulations is available. Then its values can be calculated at the required larmor frequency values and substituted to Eqs. 9 and 10 to get the R_1^C and R_1^D. The value of the effective correlation time can be calculated directly from the interated area below the correlation function, see Fig. 8 or from Eq. 30 in Ref. [23].

Comparing C–H bond dynamcis between simulations and NMR experiments

The spin lattice relaxation parameters R_1^C, R_1^D and $R_{1\rho}$ are considered as directly measurable experimental parameters and the effective correlation time τ_e can be derived directly from directly measurable parameters without further assumptions (see Eq. 11 and Ref. [23]). Spin lattice relaxation parameters R_1^C and R_1^D can be calculated from simulations by first calculating the auto–correlation function (Eq. 4), then calculating the spectral density from the Fourier transformation (Eq. 5) and finally substituting its values into Eqs. 9 and 10 (see also previous section). The effective correlation time can be calculated directly from integrated area and order parameter or from Eq. 30 in Ref. [23]. In practise, the $R_{1\rho}$ cannot be calculated from simulations directly since its value depends also on the slow relaxation dynamics ($g_s(t)$ in Eq. 6) which is not present in simulations. The same applies to the calculation of NOESY relaxations rates and in this case decay time of 170 ns was assumed for the $g_s(t)$ [110], while 4.2 ms was measured by Ferreira et al. [23].

As seen from Eqs. 9 and 10, the numerical values of R_1^C and R_1^D depend also on the carbon ω_C, hydrogen ω_H and deuterium ω_D Larmor frequencies which, in turn, depend on the spectrometer external magnetic field. From simulations it is straighforwad to calculate the spectral density with any Larmor frequncy value to get the R_1^C and R_1^D as a function of external magnetic field. However, in experiments with standard spectrometers the external field cannot be changed, i.e. each spectrometer has their specific field strengths. Thus, to measure R_1^C or R_1^D values as a function of magnetic field one has to use several spectrometers which is tedious and spectrometers excists only with limited amount of magnetic field strengths. Despite of these challenges this kind of experiments have been done and the available data is reviewed by Leftin et al. [10]. Another approach to measure the magnetic field strength depedence of spin lattice relaxation times is the Field Cycling NMR [111, 112]. However, this is not yet feasible

with standard spectrometer and only limited amount of data is available, mostly from ^{31}P NMR [111–113] but also from ^{13}C NMR [114].

The magnetic field strength dependence of spin relaxation times between simulations and experiments is compared in several studies [71, 101, 102, 104, 105, 108]. Examples of such comparison for acyl chain segments are shown in Fig. 9. On the other, some studies have compared R_1^C and R_1^D measured with one magnetic field strenght to the value calculated from simulations [23, 54, 71, 86, 89, 94]. Example of such comparison between R_1^C from simulations and experiments is shown in Fig. 10 Comparisons seems to generally show a good agreement with large larmor frequencies which is getting worse when the Larmor frequency decreases. On the other hand, the level of the agreement depends on the carbon segment and the type of relaxation used in the comparison; Berger model compared with 2H NMR gives better agreement for C_7 segment compared to C_3 (Fig. 9 B)) while comparison to 13C NMR relaxation with one frequency gives similar discrepancy for both segments (Fig. 10). For CHARMM the agreement seems better when going towards bilayer center, see Fig. 9 A). Due to the complicated connection between molecular dynamics and spin relaxation it is not straightforward to make conclusions about the dynamical differences between reality and simulations. This is, however, possible with careful analysis as discussed in the next section.

To ease the intuitive interpretation of experimentally measured rotational dynamics Ferreira et al. showed that the effective correlation time can be measured by combining directly measurable quantities without any assumptions on dynamical prosesses present in the fast relaxation regime [23]. The comparison of effective correlation times between experiments and simulations for different segments is shown in Fig. 10. From this result it is straightforward to conclude that acyl chain rotational dynamics is generally well described while in the interfacial region, especially in glycerol backbone, the dynamics is too slow in simulations. It should be noted, however, that the effective correlation describes the total relaxation over all short timescales present in $g_f(t)$. Even if this is correct, the balance between different processes with different relaxatio times may not be correct. This is actually seen in the acyl chains, where R_1 does not perfectly agree with experiments while τ_e does.

Interplay between simulations and NMR spin lattice relaxation times: Validation and interpretation of dynamics

By measuring single spin relaxation time values it is almost impossible to make any conclusions about molecular dynamics due to their complicated connection through the spectral density. Even changes of relaxation times cannot be directly related to molecular dynamics without further information since, e.g. faster dynamics may lead to the decrease or increase of spin relaxation times, depending on the other dynamics processes present and the used magnetic field strength
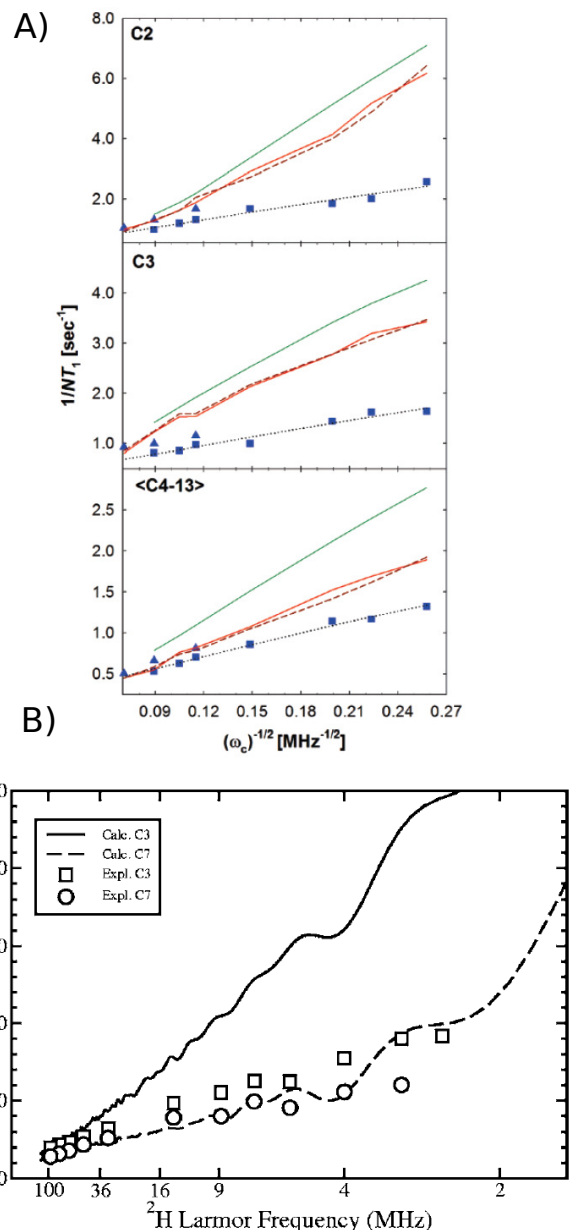

FIG. 9: A) Comparison of R_1^C dependence on magnetic field between experiments and CHARMM simulations for acyl chain carbons (DPPC bilayer in 323K) adapted from [108]. Experiments as points; MD simulations as solid and dashed lines; and a model-free fit to the vesicle data as dotted lines. B) Comparison of R_1^D dependence on magnetic field between experiments and Berger simulations for acyl chain carbons (DMPC bilayer in 300K) adapted from [102].

as demonstrated, for example in [23].

Careful studies of spin relaxation times as a function of temperature and magnetic field to overcome this issue are recently reviewed by Leftin and Brown [10]. From compilation of different experimental data sets it was possible to conclude, for example, that the interfacial region of lipid molecules has slower dynamics than acyl chains [10]. Another successfull
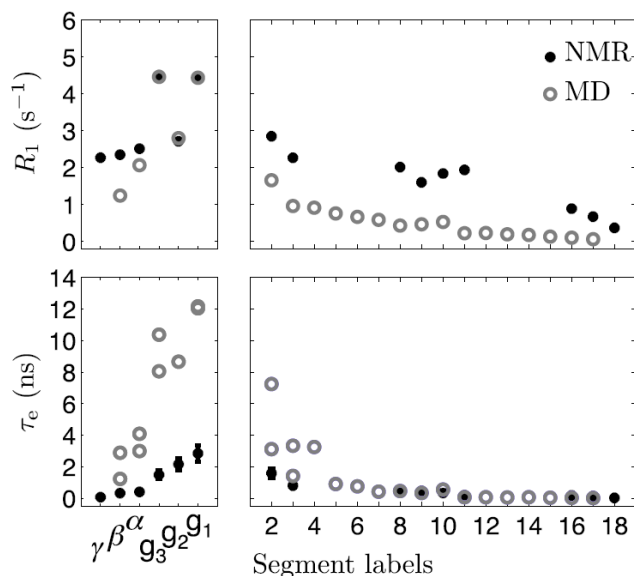
FIG. 10: (top) R_1^C for POPC bilayer in 298K calculated from simulations with Berger model compared to experimental results measured with field strength correspondin to the Larmor frequency of 125 MHz for ^{13}C. (bottom) Effective correlation times for the same system compared between simulations and experiments. Figure adapted from Ferreira et al. [23].

approach to interpret the spin relaxation times has been to use the atomistic resolution molecular dynamics simulations to reproduce the measured changes and then analyze the dynamical changes from the simulation trajectory [86, 94, 115]. This approach has been especially useful in the studies of polyunsaturated acyl chain dynamics which concluded by combining the simulation and NMR relaxation data that the double bonds speed us the chain dynamics due to flexible dihedrals next to the double bonds [86, 94–96].

To ease the interpretation of the measured spin relaxation times Ferreira et al. recently introduced a model free connection between effective correlation time and directly measurable spin relaxation rates [23]. The main advantages of effective correlation time is that its connection to molecular dynamics is straightforward in the sense that the general dynamics is faster when effective correlation time decreases and *vice versa* and that it can be quantitatively compared to simulations. As shown in Fig. 10 these experiments immediately show that the glycerol backbone has the slowest dynamics of lipid segments (in agreement with conclusions from the combination of several previous experimental sets [10]) and that the dynamics of these is significantly underestimated by the Berger model.

Most importantly, the rough agreement of spin relaxation rates and effective correlation times between simulations and experiments shows that the rotational dynamical processes present in simulations has the correct order of magnitude [23, 54, 71, 71, 86, 89, 94, 101, 102, 104, 105, 108].

Consequently, the dynamical visualizations of simulation trajectories (videos) can be considered as a realistic intuitive presentations of lipid bilayers. However, in more detailed studies it should be kept in mind that all the dynamical (and also structural) details are not exactly correct.

The lipid rotational dynamics has been often interpreted by using the so called wobble in the cone model [104, 105, 108, 109, 114]. The main idea of the model is that the whole lipid molecule is wobbling as a cone such that all the all the segments share the time scale for this wobbling. In addition, each segments have further timescales related to their dynamincs inside the cone. The auto–correlation functions assuming the wobble in the cone model can be nicely fit to the simulation data and also some experimental results can be reproduced. However, also auto–correlation functions having different type of dynamics can be used to do the same. On the other hand, it has been recently pointed out that significant changes of structure and dynamics experienced in acyl chain region may not reflect to the headgroup [15, 116] indicating weak coupling between these segments. This idea is also in line with one possible interpretation of recent field cycling experiments [113]. In addition, the role of undulations in the relaxation data measured with low frequencies is under discussion [10, 107–109].

In conclusion, the timescale of rotational dynamics is correct in simulations while the exact correlation times and relaxation processes are not fully reproduced. More experimental and simulation studies are needed to fully understand current quality of dynamics in current models. To interpretate the relaxation prcosesses present in lipid bilayer, a model which can be shown to agree with experiments on all fast timescales is needed.

STUCTURE FACTORS FROM SCATTERING AND SIMULATIONS

For this section I would be more than happy for some help

Here will be described:

How are the form factors are measured.
What is the primary experimental observable.

On these questions I do not know the answer and it is not exactly clear from where I can find the answers. More specifically:

8.Which is the experimental quantity that the scattering machinary exatcly puts out?

How the form factor is determined from the experimental observables?

Which assumptions are needed here?

There is already some discussion about this in the blog by Peter Heftberger and Georg Pabst, but any kind of information from full exaplanation with citations to the hints of relevant literature are helpful here. The more detailed discussion can be found at: `https://github.com/NMRLipids/NMRLipids_V-Review/issues/1`

How accurate are the experimental form factors.

9.Has this been discussed in the literature already? Any kind of information from full exaplanation with citations to the hints of relevant literature are helpful here. The more detailed discussion can be found at: `https://github.com/NMRLipids/NMRLipids_V-Review/issues/2`

How the form factor is calculated from simulations and compared to experimental ones.

10.As far as I have understood, the form factor is simply a Fourier transform of electron density. I have some quick and dirty scripts to calculate those in the NMRLipids III repository:

`https://github.com/NMRLipids/NmrLipidsCholXray/blob/master/scratch/FFactor/FFstructCALC.sh`

`https://github.com/NMRLipids/NmrLipidsCholXray/tree/master/scratch/FFactor`

However, I have not been able to install the SIMtoEXP program (`http://link.springer.com/article/10.1007%2Fs00232-010-9254-5`) so I have not been able to check my script against the standard method. This should be straighforward issue and should become clear once I check the details. Anyway, any kind of information from full exaplanation with citations to the hints of relevant literature are helpful here. The more detailed discussion can be found at: `https://github.com/NMRLipids/NMRLipids_V-Review/issues/3`

How accurate are the calculated form factors from simulations.

11.I think that from statistical point of view accuracy is quite high, however I am not sure about the effect of undulations etc. Any kind of information from full exaplanation with citations to the hints of relevant literature are helpful here. The more detailed discussion can be found at: `https://github.com/NMRLipids/NMRLipids_V-Review/issues/4`

What can be learned about the structure when comparing the form factors between experiments and simulations

12.I have thought that if the form factor is reproduced by the simulation, the electron density profile should be reasonable. However, since some people are tuning the peak highs for better agreement, I am not sure. There is also some connection to the thickness. There is already some discussion about this in the blog with Peter Heftberger and Georg Pabst. Any kind of information from full exaplanation with citations to the hints of relevant literature are helpful here. The more detailed discussion can be found at: `https://github.com/NMRLipids/NMRLipids_V-Review/issues/5`

CONCLUSIONS

---

* `samuli.ollila@aalto.fi`

[1] A. Abragam, *The Principles of Nuclear Magnetism* (Oxford University Press, 1961).

[2] H. U. Gally, W. Niederberger, and J. Seelig, Biochemistry **14**, 3647 (1975).

[3] A. Seelig and J. Seelig, Biochemistry **16**, 45 (1977).

[4] J. Seelig and N. Waespe-Sarcevic, Biochemistry **17**, 3310 (1978).

[5] L. Strenk, P. Westerman, and J. Doane, Biophys. J. **48**, 765 (1985).

[6] J. E. Baenziger, H. C. Jarrel, R. J. Hill, and I. C. P. Smith, Biochemistry **30**, 894 (1991).

[7] M. Hong, K. Schmidt-Rohr, and D. Nanz, Biophys. J. **69**, 1939 (1995).

[8] J. Chowdhary, E. Harder, P. E. M. Lopes, L. Huang, A. D. MacKerell, and B. Roux, J. Phys. Chem. B **117**, 9142 (2013).

[9] P. Prakash and R. Sankararamakrishnan, J. Comp. Chem. **31**, 266 (2010).

[10] A. Leftin and M. F. Brown, Biochim. Biophys. Acta - Biomembranes **1808**, 818 (2011).

[11] D. Marsh, *Handbook of Lipid Bilayers, Second Edition* (RSC press, 2013).

[12] S. V. Dvinskikh, V. Castro, and D. Sandstrom, Phys. Chem. Chem. Phys. **7**, 607 (2005).

[13] Journal of Molecular Biology **425**, 2973 (2013).

[14] A. Leftin, T. Molugu, C. Job, K. Beyer, and M. Brown, Biophysical Journal **107**, 2274 (2014).

[15] A. Botan, F. Fernando, J. F. Patrick Franois, M. Javanainen, M. Kanduc, W. Kulig, A. Lamberg, C. Loison, A. P. Lyubartsev, M. S. Miettinen, et al., The Journal of Physical Chemistry B **0**, null (0), pMID: 26509669, http://dx.doi.org/10.1021/acs.jpcb.5b04878, URL `http://dx.doi.org/10.1021/acs.jpcb.5b04878`.

[16] J. Seelig, Q. Rev. Biophys. **10**, 353 (1977).

[17] M. Hong, K. Schmidt-Rohr, and A. Pines, J. Am. Chem. Soc. **117**, 3310 (1995).

[18] J. D. Gross, D. E. Warschawski, and R. G. Griffin, J. Am. Chem. Soc. **119**, 796 (1997).

[19] T. M. Ferreira, F. Coreta-Gomes, O. H. S. Ollila, M. J. Moreno, W. L. C. Vaz, and D. Topgaard, Phys. Chem. Chem. Phys. **15**, 1976 (2013).

[20] H. U. Gally, G. Pluschke, P. Overath, and J. Seelig, Biochemistry **20**, 1826 (1981).

[21] A. K. Engel and D. Cowburn, FEBS Letters **126**, 169 (1981).

[22] J. Becker, A. Comotti, R. Simonutti, P. Sozzani, and K. Saalwchter, The Journal of Physical Chemistry B **109**, 23285 (2005).

[23] T. M. Ferreira, O. H. S. Ollila, R. Pigliapochi, A. P. Dabkowska, and D. Topgaard, J. Chem. Phys. **142**, 044905 (2015), URL `http://scitation.aip.org/content/aip/journal/jcp/142/4/10.1063/1.4906274`.

[24] D. Warschawski and P. Devaux, Eur. Biophys. J. **34**, 987 (2005), ISSN 0175-7571.

[25] H. Akutsu and J. Seelig, Biochemistry **20**, 7366 (1981).

[26] B. Bechinger and J. Seelig, Chem. Phys. Lipids **58**, 1 (1991).

[27] O. Berger, O. Edholm, and F. Jähnig, Biophys. J. **72**, 2002 (1997).

[28] C.-J. Högberg, A. M. Nikitin, and A. P. Lyubartsev, J. Comput. Chem. **29**, 2359 (2008).

[29] D. Poger, W. F. Van Gunsteren, and A. E. Mark, J. Comput. Chem. **31**, 1117 (2010).

[30] J. P. Ulmschneider and M. B. Ulmschneider, J. Chem. Theory Comput. **5**, 1803 (2009).

[31] A. Kukol, J. Chem. Theory Comput. **5**, 615 (2009).

[32] S.-W. Chiu, S. A. Pandit, H. L. Scott, and E. Jakobsson, J. Phys. Chem. B **113**, 2748 (2009).

[33] J. B. Klauda, R. M. Venable, J. A. Freites, J. W. O'Connor, D. J. Tobias, C. Mondragon-Ramirez, I. Vorobyov, A. D. M. Jr, and R. W. Pastor, J. Phys. Chem. B **114**, 7830 (2010).

[34] C. J. Dickson, L. Rosso, R. M. Betz, R. C. Walker, and I. R. Gould, Soft Matter **8**, 9617 (2012).

[35] J. P. M. Jämbeck and A. P. Lyubartsev, J. Phys. Chem. B **116**, 3164 (2012).

[36] A. Maciejewski, M. Pasenkiewicz-Gierula, O. Cramariuc, I. Vattulainen, and T. Rog, J. Phys. Chem. B **118**, 4571 (2014).

[37] R. Tjörnhammar and O. Edholm, J. Chem. Theory Comput. **10**, 5706 (2014).

[38] C. J. Dickson, B. D. Madej, . A. Skjevik, R. M. Betz, K. Teigen, I. R. Gould, and R. C. Walker, J. Chem. Theory Comput. **10**, 865 (2014).

[39] S. Lee, A. Tran, M. Allsopp, J. B. Lim, J. Henin, and J. B. Klauda, J. Phys. Chem. B **118**, 547 (2014).

[40] B. Perly, I. C. P. Smith, and H. C. Jarrell, Biochemistry **24**, 1055 (1985).

[41] S. V. Dvinskikh, V. Castro, and D. Sandstrom, Phys. Chem. Chem. Phys. **7**, 3255 (2005).

[42] A. Ulrich and A. Watts, Biophys. J. **66**, 1441 (1994).

[43] M. F. Brown and J. Seelig, Biochemistry **17**, 381 (1978).

[44] F. Aussenac, M. Laguerre, J.-M. Schmitter, and E. J. Dufourc, Langmuir **19**, 10468 (2003).

[45] C. Altenbach and J. Seelig, Biochemistry **23**, 3913 (1984).

[46] J. Seelig, P. M. MacDonald, and P. G. Scherer, Biochemistry **26**, 7535 (1987).

[47] G. Raffard, S. Steinbruckner, A. Arnold, J. H. Davis, and E. J. Dufourc, Langmuir **16**, 7655 (2000).

[48] C. R. Sanders and J. P. Schwonek, Biochemistry **31**, 8898 (1992).

[49] L. E. Marbella, B. Yin, and M. M. Spence, The Journal of Physical Chemistry B **119**, 4194 (2015).

[50] K. Mallikarjunaiah, A. Leftin, J. J. Kinnun, M. J. Justice, A. L. Rogozea, H. I. Petrache, and M. F. Brown, Biophysical Journal **100**, 98 (2011), ISSN 0006-3495, URL `http://www.sciencedirect.com/science/article/pii/S0006349510013792`.

[51] A. Catte, M. Girych, M. Javanainen, M. S. Miettinen, L. Monticelli, J. Määttä, V. S. Oganesyan, and O. H. S. Ollila, *The electrometer concept and binding of cations to phospholipid bilayers* (2015), dOI: 10.5281/zenodo.32175.

[52] M. Roux, J. M. Neumann, R. S. Hodges, P. F. Devaux, and M. Bloom, Biochemistry **28**, 2313 (1989).

[53] E. Kuchinka and J. Seelig, Biochemistry **28**, 4216 (1989).

[54] S. Ollila, M. T. Hyvönen, and I. Vattulainen, J. Phys. Chem. B **111**, 3139 (2007).

[55] L. Vermeer, B. de Groot, V. Rat, A. Milon, and J. Czaplicki, Eur. Biophys. J. **36**, 919 (2007), ISSN 0175-7571, URL `http://dx.doi.org/10.1007/s00249-007-0192-9`.

[56] D. P. Tieleman, S. J. Marrink, and H. J. C. Berendsen, Biochim. Biophys. Acta **1331**, 235 (1997).

[57] D. Poger and A. E. Mark, J. Chem. Theory Comput. **8**, 4807 (2012).

[58] M. Bachar, P. Brunelle, D. P. Tieleman, and A. Rauk, J. Phys. Chem. B **108**, 7170 (2004).

[59] J. Wong-ekkabut, Z. Xu, W. Triampo, I.-M. Tang, D. P. Tieleman, and L. Monticelli, Biophysical Journal **93**, 4225 (2007), ISSN 0006-3495, URL http://www.sciencedirect.com/science/article/pii/S0006349507716752.

[60] A. Vogel and S. Feller, The Journal of Membrane Biology **245**, 23 (2012), ISSN 0022-2631.

[61] P. van der Ploeg and H. J. C. Berendsen, The Journal of Chemical Physics **76** (1982).

[62] E. Egberts and H. J. C. Berendsen, J. Chem. Phys. **89**, 3718 (1988).

[63] T. R. Stouch, Molecular Simulation **10**, 335 (1993).

[64] E. Egberts, S.-J. Marrink, and H. Berendsen, European Biophysics Journal **22**, 423 (1994), ISSN 0175-7571, URL http://dx.doi.org/10.1007/BF00180163.

[65] J. W. Essex, M. M. Hann, and W. G. Richards, Philos. T. Roy. Soc. B **344**, 239 (1994).

[66] A. Robinson, W. Richards, P. Thomas, and M. Hann, Biophys. J. **67**, 2345 (1994).

[67] M. T. Hyvönen, M. Ala-Korpela, J. Vaara, T. T. Rantala, and J. Jokisaari, Chem. Phys. Lett. **246**, 300 (1995).

[68] V. Kothekar, Ind. J. Biochem. Biophys. **33**, 431 (1996).

[69] D. P. Tieleman and H. J. C. Berendsen, J. Chem. Phys. **105**, 4871 (1996).

[70] W. Shinoda, N. Namiki, and S. Okazaki, J. Chem. Phys. **106**, 5731 (1997).

[71] J. B. Klauda, R. M. Venable, A. D. M. Jr., and R. W. Pastor, in *Computational Modeling of Membrane Bilayers*, edited by S. E. Feller (Academic Press, 2008), vol. 60 of *Current Topics in Membranes*, pp. 1 – 48.

[72] M. Lafleur, P. Cullis, and M. Bloom, European Biophysics Journal **19**, 55 (1990), ISSN 0175-7571, URL http://dx.doi.org/10.1007/BF00185086.

[73] J. A. Urbina, S. Pekerar, H. biao Le, J. Patterson, B. Montez, and E. Oldfield, Biochimica et Biophysica Acta (BBA) - Biomembranes **1238**, 163 (1995), ISSN 0005-2736, URL http://www.sciencedirect.com/science/article/pii/000527369500117L.

[74] R. J. Mashl, H. L. Scott, S. Subramaniam, and E. Jakobsson, Biophys. J. **81**, 3005 (2001).

[75] C.-J. Hgberg, , and A. P. Lyubartsev*, The Journal of Physical Chemistry B **110**, 14326 (2006).

[76] Q. Zhu, K. H. Cheng, and M. W. Vaughn, J. Phys. Chem. B **111**, 11021 (2007).

[77] J. B. Lim, B. Rogaski, and J. B. Klauda, J. Phys. Chem. B **116**, 203 (2012).

[78] J. P. M. Jambeck and A. P. Lyubartsev, Phys. Chem. Chem. Phys. **15**, 4677 (2013).

[79] B. D. Madej, I. R. Gould, and R. C. Walker, The Journal of Physical Chemistry B **119**, 12424 (2015).

[80] M. Höltje, T. Förster, B. Brandt, T. Engels, W. von Rybinski, and H.-D. Höltje, Biochim. Biophys. Acta **1511**, 156 (2001).

[81] M. T. Hyvönen, T. T. Rantala, and M. Ala-Korpela, Biophys. J. **73**, 2907 (1997).

[82] M. Hyvnen, M. Ala-Korpela, J. Vaara, T. T. Rantala, and J. Jokisaari, Chemical Physics Letters **268**, 55 (1997), ISSN 0009-2614, URL http://www.sciencedirect.com/science/article/pii/S0009261497001711.

[83] S. Feller, D. Yin, R. Pastor, and A. M. Jr, Biophysical Journal **73**, 2269 (1997).

[84] L. Saiz and M. L. Klein, Biophys. J. **204**, 204 (2001).

[85] T. Huber, K. Rajamoorthi, V. F. Kurze, K. Beyer, and M. F. Brown, J. Am. Chem. Soc. **124**, 298 (2002).

[86] S. E. Feller, K. Gawrisch, and A. D. MacKerell Jr., J. Am. Chem. Soc. **124**, 318 (2002).

[87] T. Rg, K. Murzyn, R. Gurbiel, Y. Takaoka, A. Kusumi, and M. Pasenkiewicz-Gierula, Journal of Lipid Research **45**, 326 (2004).

[88] M. T. Hyvönen and P. T. Kovanen, Eur. Biophys. J. **34**, 294 (2005).

[89] J. B. Klauda, V. Monje, T. Kim, and W. Im, The Journal of Physical Chemistry B **116**, 9424 (2012).

[90] W. Kulig, M. Pasenkiewicz-Gierula, and T. Róg, Chem. Phys. Lipids pp. *In Press, Accepted Manuscript, http://dx.doi.org/10.1016/j.chemphyslip.2015.07.002* (2015), URL http://www.sciencedirect.com/science/article/pii/S0009308415300074.

[91] H. I. Petrache, S. W. Dodd, and M. F. Brown, Biophys. J. **79**, 3172 (2000).

[92] K. Rajamoorthi and M. F. Brown, Biochemistry **30**, 4204 (1991).

[93] J. Kapla, B. Stevensson, M. Dahlberg, and A. Maliniak, J. Phys. Chem. B **116**, 244 (2012).

[94] N. V. Eldho, S. E. Feller, S. Tristram-Nagle, I. V. Polozov, and K. Gawrisch, J. Am. Chem. Soc. **125**, 6409 (2003).

[95] W. Stillwell and S. R. Wassall, Chem. Phys. Lipids **126**, 1 (2003).

[96] K. Gawrisch, N. V. Eldho, and L. L. Holte, Lipids **38**, 445 (2003).

[97] J. H. Ipsen, G. Karlstrm, O. Mourtisen, H. Wennerstrm, and M. Zuckermann, Biochimica et Biophysica Acta (BBA) - Biomembranes **905**, 162 (1987).

[98] G. Lipari and A. Szabo, J. Am. Chem. Soc. **104**, 4546 (1982).

[99] A. Nowacka, P. C. Mohr, J. Norrman, R. W. Martin, and D. Topgaard, Langmuir **26**, 16848 (2010).

[100] J. Hirschinger, Concept. Magn. Reson. A **28A**, 307 (2006).

[101] E. Lindahl and O. Edholm, J. Chem. Phys. **115**, 4938 (2001).

[102] J. Wohlert, W. K. den Otter, O. Edholm, and W. J. Briels, J. Chem. Phys. **124**, 154905 (2006).

[103] M. Abraham, D. van der Spoel, E. Lindahl, B. Hess, and the GROMACS development team, *GROMACS user manual version 5.0.7* (2015), URL www.gromacs.org.

[104] R. W. Pastor, R. M. Venable, M. Karplus, and A. Szabo, The Journal of Chemical Physics **89** (1988).

[105] R. W. Pastor*, , R. M. Venable, and S. E. Feller, Accounts of Chemical Research **35**, 438 (2002).

[106] R. Venable, Y. Zhang, B. Hardy, and R. Pastor, Science **262**, 223 (1993).

[107] O. Edholm, in *Computational Modeling of Membrane Bilayers*, edited by S. E. Feller (Academic Press, 2008), vol. 60 of *Current Topics in Membranes*, pp. 91 – 110.

[108] J. B. Klauda, N. V. Eldho, , K. Gawrisch, B. R. Brooks, , and R. W. Pastor*, The Journal of Physical Chemistry B **112**, 5924 (2008).

[109] J. B. Klauda, M. F. Roberts, A. G. Redfield, B. R. Brooks, and R. W. Pastor, Biophysical Journal **94**, 3074 (2008), ISSN 0006-3495, URL `http://www.sciencedirect.com/science/article/pii/S0006349508704648`.

[110] S. E. Feller, D. Huster, , and K. Gawrisch, Journal of the American Chemical Society **121**, 8963 (1999).

[111] M. F. Roberts, , and . Alfred G. Redfield*, Journal of the American Chemical Society **126**, 13765 (2004).

[112] M. F. Roberts and A. G. Redfield, Proceedings of the National Academy of Sciences of the United States of America **101**, 17066 (2004).

[113] M. F. Roberts, A. G. Redfield, and U. Mohanty, Biophys. J. **97**, 132 (2009).

[114] V. N. Sivanandam, J. Cai, A. G. Redfield, and M. F. Roberts, Journal of the American Chemical Society **131**, 3420 (2009).

[115] A. Nowacka, N. Bongartz, O. Ollila, T. Nylander, and D. Topgaard, Journal of Magnetic Resonance **230**, 165 (2013).

[116] T. M. Ferreira, Ph.D. thesis, Lund University, http://lup.lub.lu.se/record/3878850/file/3879121.pdf (2013).

[117] P. G. Scherer and J. Seelig, Biochemistry **28**, 7720 (1989).

[118] These changes were later shown to be consistent with the addition of different charges into the bilayer, and the electrometer concept was introduced to measure the amount of charge incorporated in the bilayer interface [117].

[119] This increase is related to the P-N vector tilting more parallel to the membrane plane [15] which is in agreement with electrometer concept suggesting that penetrating charge has opposite effect on headgroup tilt leading to decrease of order parameters [51, 117].

[120] In this work CH_2/CH_3 groups in cholesterol were changed to LP_2/LP_3 groups to make it more consistent with the Berger parameters. This is not usually done in the studies done with these model.

ToDo

P.

1. Samuli: Add citations to the introduction. Rewriting is also needed 1

2. References should be added, the text should polished, things should be added and checked and figures should be improved. However, the main strucutre and idea of the section should be visible. 2

3. How accurate exactly? 3

4. Maybe specify to which ones? 3

5. Has this been done for the C_2 carbon in the *sn*-2 chain? 6

6. The analysis with ions not actually done yet! 9

7. This is the first sketch of this section. A lot of references should be added, the text should polished, things should be added and checked and figures should be improved. However, the main strucutre and idea of the section should be visible. 10

8. Which is the experimental quantity that the scattering machinary exatcly puts out? How the form factor is determined from the experimental observables? Which assumptions are needed here? There is already some discussion about this in the blog by Peter Heftberger and Georg Pabst, but any kind of information from full exaplanation with citations to the hints of relevant literature are helpful here. The more detailed discussion can be found at: `https://github.com/NMRLipids/NMRLipids_V-Review/issues/1` 15

9. Has this been discussed in the literature already? Any kind of information from full exaplanation with citations to the hints of relevant literature are helpful here. The more detailed discussion can be found at: `https://github.com/NMRLipids/NMRLipids_V-Review/issues/2` 15

10. As far as I have understood, the form factor is simply a Fourier transform of electron density. I have some quick and dirty scripts to calculate those in the NMRLipids III repository: `https://github.com/NMRLipids/NmrLipidsCholXray/blob/master/scratch/FFactor/FFstructCALC.sh` `https://github.com/NMRLipids/NmrLipidsCholXray/tree/master/scratch/FFactor` However, I have not been able to install the SIMtoEXP program (`http://link.springer.com/article/10.1007%2Fs00232-0` so I have not been able to check my script against the standard method. This should be straighforward issue and should become clear once I check the details. Anyway, any kind of information from full exaplanation with citations to the hints of relevant literature are helpful here. The more detailed discussion can be found at: `https://github.com/NMRLipids/NMRLipids_V-Review/issues/3` 15

11. I think that from statistical point of view accuracy is quite high, however I am not sure about the effect of undulations etc. Any kind of information from full exaplanation with citations to the hints of relevant literature are helpful here. The more detailed discussion can be found at: `https://github.com/NMRLipids/NMRLipids_V-Review/issues/4` 15

12. I have thought that if the form factor is reproduced by the simulation, the electron density profile should be reasonable. However, since some people are tuning the peak highs for better agreement, I am not sure. There is also some connection to the thickness. There is already some discussion about this in the blog with Peter Heftberger and Georg Pabst. Any kind of information from full exaplanation with citations to the hints of relevant literature are helpful here. The more detailed discussion can be found at: `https://github.com/NMRLipids/NMRLipids_V-Review/issues/5` 15